Archives of Materials Science and Engineering

Volume 111
Issue 2
October 2021
Pages 66-77

International Scientific Journal
published monthly by the
World Academy of Materials
and Manufacturing Engineering

DOI: 10.5604/01.3001.0015.5806

Effect of infill and density pattern on the mechanical behaviour of ABS parts manufactured by FDM using Taguchi and ANOVA approach

M. Othmani [a,*], K. Zarbane [b], A. Chouaf [a]

[a] National School of Electricity and Mechanics, Hassan II University of Casablanca, B.P 8118 Oasis, Casablanca, Morocco

[b] Casablanca Higher School of Technology, Hassan II University of Casablanca, B.P 8012 Oasis, Casablanca, Morocco

* Corresponding e-mail address: othmani.mourad@gmail.com

ORCID identifier: https://orcid.org/0000-0001-8601-8073 (M.O.);
https://orcid.org/0000-0002-6048-5279 (K.Z.);
https://orcid.org/0000-0003-1765-6762 (A.C.)

ABSTRACT

Purpose: The present work aims to investigate the effect of many infill patterns (rectilinear, line, grid, triangles, cubic, concentric, honeycomb, 3D honeycomb) and the infill density on the mechanical tensile strength of an Acrylonitrile Butadiene Styrene (ABS) test specimen manufactured numerically by FDM.

Design/methodology/approach: Computer-Aided Design (CAD) software has been used to model the geometry and the mesostructure of the test specimens in a fully automatic manner from a G-code file by using a script. Then, a Numerical Design of Experiments (NDoE) has been carried out by using Taguchi method and the Analysis of Variance (ANOVA). The tensile behaviour of these numerical test specimens has been studied by the Finite Element Analysis (FEA).

Findings: The FEA results showed that a maximal Ultimate Tensile Strength (UTS) was reached by using the 'concentric' infill pattern combined with an infill density of 30%. The results also show that the infill pattern and the infill density are significant factors.

Research limitations/implications: The low infill densities of 20% and 30% that have already been used in many previous studies, we have also applied it in order to reduce the time of the simulations. Indeed, with high infill density, the simulations take a very excessive time. In an ongoing study, we predicted higher percentages.

Practical implications: This study provided an important modelling tool for the design and manufacture of functional parts and helps the FDM practitioners and engineers to manufacture strong and lightweight FDM parts by choosing the optimal process parameters.

Originality/value: This study elucidated the effect of various infill patterns on the tensile properties of the test specimens and applied for the first time a NDoE using numerical test

specimens created by the mesostructured approach, which considerably minimized the cost of the experiments while obtaining an error of 6.8% between the numerical and the experimental values of the UTS.

Keywords: Fused deposition modelling, Infill pattern, Infill density, Finite element analysis, Taguchi

Reference to this paper should be given in the following way:

M. Othmani, K. Zarbane, A. Chouaf, Effect of infill and density pattern on the mechanical behaviour of ABS parts manufactured by FDM using Taguchi and ANOVA approach, Archives of Materials Science and Engineering 111/2 (2021) 66-77.

DOI: https://doi.org/10.5604/01.3001.0015.5806

METHODOLOGY OF RESEARCH, ANALYSIS AND MODELLING

1. Introduction

Fused Deposition Modelling (FDM) technology is the Additive Manufacturing (AM) technology that allows the realization of complex shaped parts at the lowest cost. Compared to subtractive technologies, FDM is the most economical in small series manufacturing. FDM has many applications in the industrial field. For example, it is used for the manufacturing of scaffolds and implants for biomedical applications by employing biodegradable materials, and the manufacturing of strong components with a low infill density for automobile and aerospace interiors using thermoplastic materials such as the Acrylonitrile Butadiene Styrene (ABS) [1-3]. These components are lightweight compared to those manufactured by injection moulding technology, which reduces fuel consumption. We remind that the mechanical properties and the quality of the parts manufactured by FDM technology are strongly related to the choice of the manufacturing parameters that, until nowadays, have remained less controlled. In order to optimize or to improve the properties and the quality of these parts, many studies have been carried out. These studies, based mainly on the experimental approaches by using a Design of Experiments (DoE) methodology [4-7], have shown that the mechanical properties depend on the process parameters. Fernandez-Vicente et al. [8] have studied experimentally the influence of the infill patterns (rectilinear, honeycomb and line) and the density of ABS parts on the tensile strength and the elastic modulus. They have found that changing the infill pattern has caused little variation (less than 5%) in the Ultimate Tensile Strength (UTS) whereas the infill density has considerably impacted the UTS. Alvarez et al. [9] experimentally analysed the influence of the infill pattern on the mechanical strength of ABS parts manufactured by FDM. They found that the maximum tensile stress can be obtained when using an infill density of 100%. Qattawi et al. [10] have investigated the effect of the layer thickness, build orientation, print speed, extrusion temperature, infill density and some infill patterns (linear, honeycomb and diamond) on the mechanical properties of Polylactic Acid (PLA) parts. They have shown the importance of the infill patterns and have obtained an error of 9.2434% and 19.0% between experimental and numerical results. Zhou et al. [11] have explored, experimentally and numerically, the effect of three infill patterns (rectilinear, honeycomb and triangular) and the infill density on the mechanical behaviour of PLA parts made by FDM. They have shown that a good UTS-to-weight ratio can be obtained when using triangular infill pattern and minimal air gaps. Their mesostructured approach has predicted some mechanical characteristics with good accuracy. Lubombo and Huneault [12] have investigated the stiffness and strength of 3D printed cellular PLA parts. They have found that varying the type of infill patterns (hexagonal, triangular, square, square-diagonal, reinforced square-diagonal) can increase significantly the stiffness and the strength. Dave et al. [13] have explored the effect of the part build orientation experimentally, infill density and infill patterns on the UTS of 3D printed PLA specimens. They have observed that tensile strength is better for concentric and rectilinear infill patterns. Yadav et al. [2] have adopted an experimental method by using FDM technology in order to design and analyse ABS parts. They studied two parameters which are the infill pattern (rectilinear and gyroid) and part build orientation. They observed that these parameters affect the mechanical strength of parts. In general, the authors have shown the importance of the infill pattern and density on the mechanical behaviour of FDM parts but their studies did not cover all the infill patterns. In addition, combinations with this parameter are little studied. Indeed, finding the right combination of the manufacturing parameters that give good mechanical properties requires a very large number of physical experiments. However, this approach is tedious and very expensive. Hence, a numerical approach should be

adopted. In this article, the tensile mechanical behaviour of ABS specimens manufactured numerically by FDM technology according to the ASTM D3039 [14] standard has been studied by using a Taguchi Numerical Design of Experiments (NDoE). For this NDoE, the infill and the density pattern have been chosen as factors. In order to simulate the numerical test specimens, a mesostructure approach has been adopted. This approach that we used was developed by several authors [15-19]. In order to achieve this, the creation of the numerical model of the specimen mesostructure has been fully automated via a script developed in 'Python' language integrated in a computational code and analysed by the Finite Element Method (FEM). In order to detect the significant manufacturing parameters, the analysis of variance (ANOVA) was used. This study provides technicians and engineers with technical decision-making information in the design and manufacture of FDM parts with good mechanical performance and lightweight.

2. Material and method

2.1. Modelling the digital test specimen obtained by FDM

In order to create the digital test specimen in accordance with the FDM machine manufacturing method, two steps have been followed [19].

First, a G-code file should be created. In order to achieve this, a 3D CAD test specimen is built by a CAD software and saved in STereoLithography (STL) format. Then the software 'Slic3r' is applied. It is a slicer program that imports the created STL file and introduces the desired manufacturing parameters. This slicing software 'Slic3r' subsequently generates a G-code file which will be used later in order to make the digital test specimen.

Second, a script in 'Python,' which is a programming language integrated in the 'Abaqus' computational code, has been developed. This script executes in 'Abaqus' all the G-code file instructions in order to draw the trajectories/ toolpath and the Model of the Raster Section (MRS) (Fig. 1) in order to create virtual extrusions and thus a digital test specimen.

At the end of the script execution, a digital test specimen that mimics the geometry and the mesostructure of the physical specimen has been obtained. The approach adopted we have developed in detail in a publication (Fig. 2) [19]. Finally, the digital test specimen will be simulated in a simple tensile test by the FEA.

2.2. NDoE

The considerable development of the means of numerical computations made it possible to carry out numerical experiments, integrating physical phenomena that are difficult to perform in laboratories or very expensive. However, performing numerical simulations of all combinations of factors and their levels can take a lot of computational time. In order to reduce this time, we can simulate a few important combinations determined by a DoE. Hence the use of a NDoE.

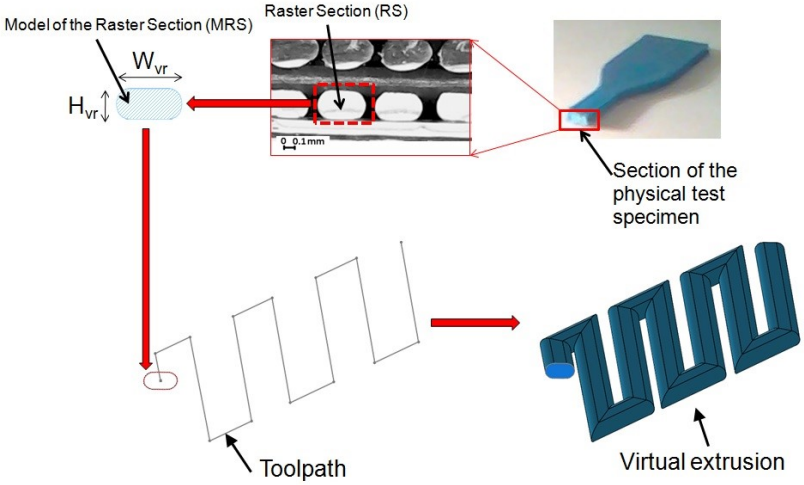

Fig. 1. Approximation of the RS from a microscopic image of a strand cross section and assigning the MRS to a toolpath to create a virtual extrusion, H_{vr} – height of the MRS, W_{vr} – width of the MRS

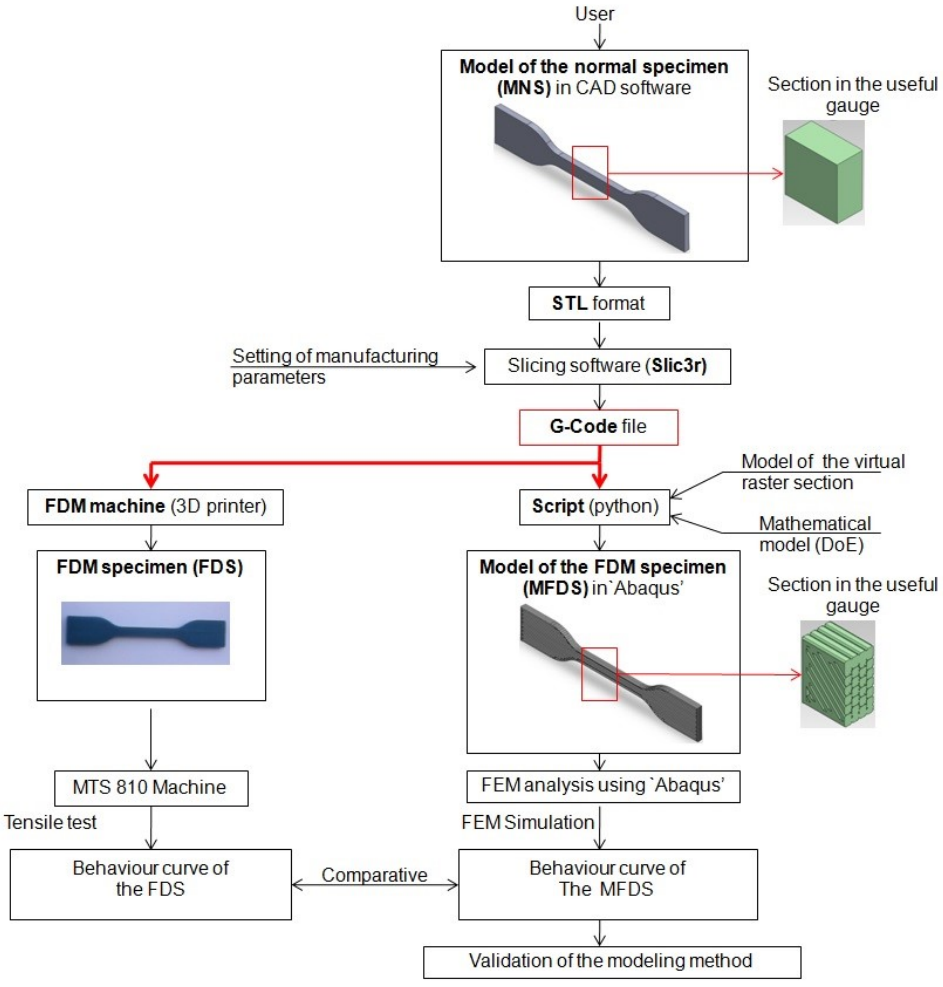

Fig. 2. Mesostructured approach for the numerical prediction of the mechanical behaviour of the FDM part

Unlike physical DoE, NDoE allows us to keep all factor levels (either controlled or fixed) fixed during numerical simulations/experiments. Thus, experimental error does not exist in all of these simulations. Therefore, repeating the tests are not useful since we will always get the same results (little dispersion of the obtained result). In this study, our method is to use a Taguchi NDoE, i.e. a Taguchi DoE which uses digital test specimens instead of physical ones.

2.3. Taguchi method

In this study, Taguchi method has been applied in order to study the main effects of process variables such as the infill pattern (Fig. 3) and the density pattern on part strength. The other parameters were kept constant. Taguchi method is used in order to achieve an optimum result with the lowest number of runs.

For this Taguchi's L16 NDoE, which requires only 8 runs, the factors and their chosen levels are listed in the Table 1. In total, sixteen numerical/digital test specimens (3D CAD) have been created according to the ASTM D3039 standard with dimensions of 127 x 12.7 x 2.54 mm (Fig. 4). This standard gives a large size of the useful area of the gage, which shows the effect of the infill patterns in the tensile test. Moreover, for our experimental and numerical tests, we have chosen the ASTM D3039 standard which has a rectangular shape since it has been reported in the literature [20,21] that, in most cases, the dumbbell shapes generate premature fractures outside the useful area of the gage of the test specimen due to the stress concentration in the curved area. This is because the 3D printer prints the curved areas in a zigzag shape as a staircase, which creates stress concentrations in these areas. In order to better highlight the importance of the infill patterns, we chose an infill density

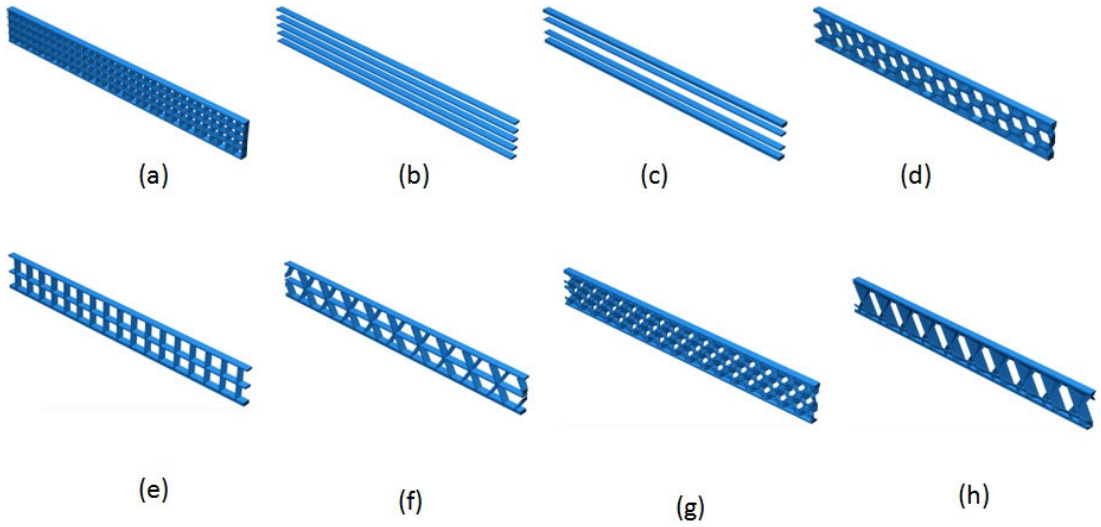

Fig. 3. Designation of infill patterns at 30% density: (a) rectilinear, (b) line, (c) concentric, (d) honeycomb, (e) grid, (f) triangles, (g) 3D honeycomb, (h) cubic

Table 1.
Factors and their level

Factor	Symbol	Level
Infill pattern	A	Concentric, line, cubic, rectilinear, honeycomb, 3D honeycomb, grid, triangles
Infill density, %	B	20, 30

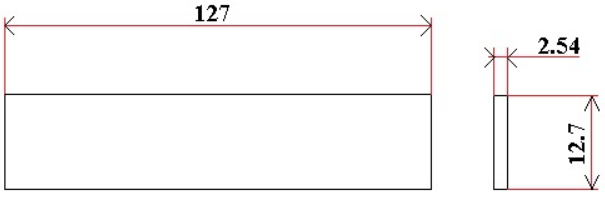

Fig. 4. The tensile test specimen as per ASTM3039 standards

of 20% and 30% [10]. These percentages have already been used in many previous studies [9,10]. We have chosen infill densities of 20% and 30% to reduce the calculation time of the simulation which is very excessive for high infill density. In a later study, we will consider higher percentages. On the other hand, we chose among those studied in the literature [8,13, 22-26], the infill patterns which presented the best mechanical resistance. The digital test specimens mimic the shape and the mesostructure of the physical test specimens which manufactured by a 3D printer.

In order to confirm the robustness of the design, signal-to-noise (S/N) ratio analysis has been conducted. The larger-the-better characteristic is chosen since the tensile strength should be maximized using the Eq. (1):

$$S/N = -10\log_{10}\left(\frac{1}{n}\sum_{i=1}^{n}\frac{1}{y^2}\right) \quad (1)$$

where 'n' is the number of experiments, and 'y_i' denotes the i-th result of the experiment.

For both NDoEs, 16 digital test specimens have been modelled according to the ASTM D3039 standard and simulated by the FEA.

The results have been discussed by using the Analysis of Variance (ANOVA) in order to determine the most influential factors.

2.4. Tensile test modelling

The behaviour of the digital test specimen previously created has been simulated through a simple tensile test by the FEA. In order to save simulation time by 'Abaqus,' the two ends held by the jaws of the traction machine have been removed [19,27]. It is worth noting that both ends are usually fixed in the jaws of the tensile machine and that the solicitation will occur in the useful area of the gage.

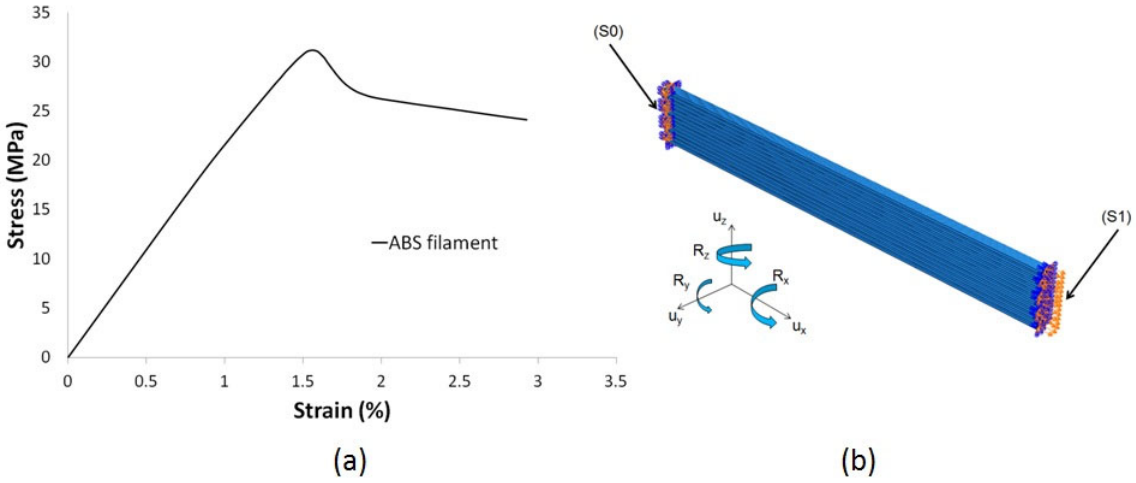

Fig. 5. a) Mechanical behavior of an ABS printed test specimen and the ABS filament [28]. b) Boundary conditions. (S0): zero displacement, (S1): imposed displacement $u_x = 10$ mm et $u_y = u_z = R_x = R_y = R_z = 0$

Furthermore, 'Tie' interaction contact type has been created between each two successive layers of the digital test specimen and between their rasters in order to stick the meshes of different nature and to prohibit the movements between the layers. According to the literature, this type of interaction has never been used in previous studies. We therefore chose this type of interaction to considerably reduce the simulation time. Then, the constitutive laws of the ABS filament feedstock carried out by Schmailzl [28] via a simple tensile test has been introduced in 'Abaqus' (Fig. 5a). From this reference, the characteristics of the filament have been extracted. Hence, for (Schmailzl [28]), the elastic modulus and Poisson's ratio are 2200 MPa and 0.3, respectively.

Concerning the boundary conditions applied in the numerical simulation, zero displacement has been added on the side (S0) of the digital test specimen while a maximum displacement has been applied on the other side (S1) along the longitudinal axis of this specimen (Fig. 5b). The value of this displacement is 10 mm.

For meshing the digital test specimen, linear 3D tetrahedral elements have been used. The size of the element is judiciously chosen in order to mesh the virtual rasters properly without increasing the simulation time. The results of the simulation are presented in the next paragraph.

2.5. Validation tests of NDoE

In order to validate the NDoE, a G-code file was created using the combination of manufacturing parameters that gives the maximum UTS. The G-code file was used to create a digital test specimen and to fabricate a physical test specimen using the RepRap Prusa i3 3D printer with ABS filament. The mechanical behaviour of the digital test specimen was simulated by the FEA, while that of the physical test specimen was obtained from the tensile test on a '3R' tensile machine with a maximum load of 25 kN. The test was carried out by imposing a displacement speed of 0.2 mm/min. Elongation of the physical specimen continued until it broke. The simultaneous acquisition of forces and displacements made it possible to plot the stress σ (in MPa) as a function of the deformation ε by considering the test specimen section of 32.258 mm^2.

In the following paragraph, the numerical results obtained from the tensile tests on the digital test specimens will be presented.

3. Results and discussion

From our numerical tensile test, the evolution of the stress as a function of the strain has been drawn in Figures 6 and 7. In this evolution, we can observe two phases of behaviour commonly mentioned in the literature. The first phase corresponds to a linear behaviour with a Young's modulus which varies from 66.89 MPa to 177.48 MPa and a yield stress which varies from 4.25 MPa to 12.3 MPa. The second phase of these curves is nonlinear through which the strain evolves under a more or less stable stress. The strain differs from one type of infill pattern to another.

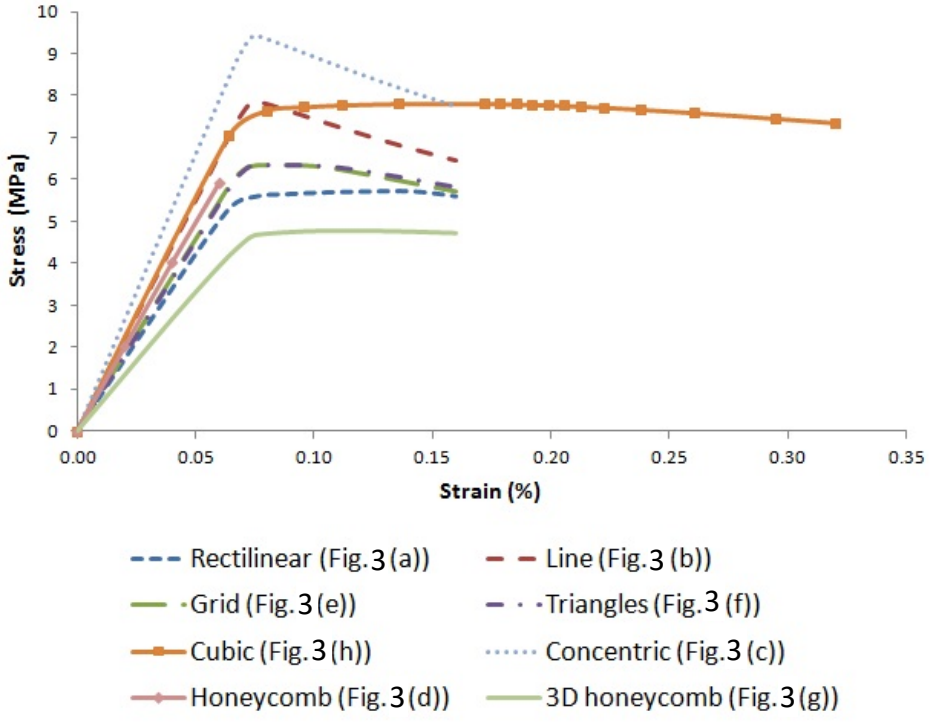

Fig. 6. Stress versus strain for infill density of 20%

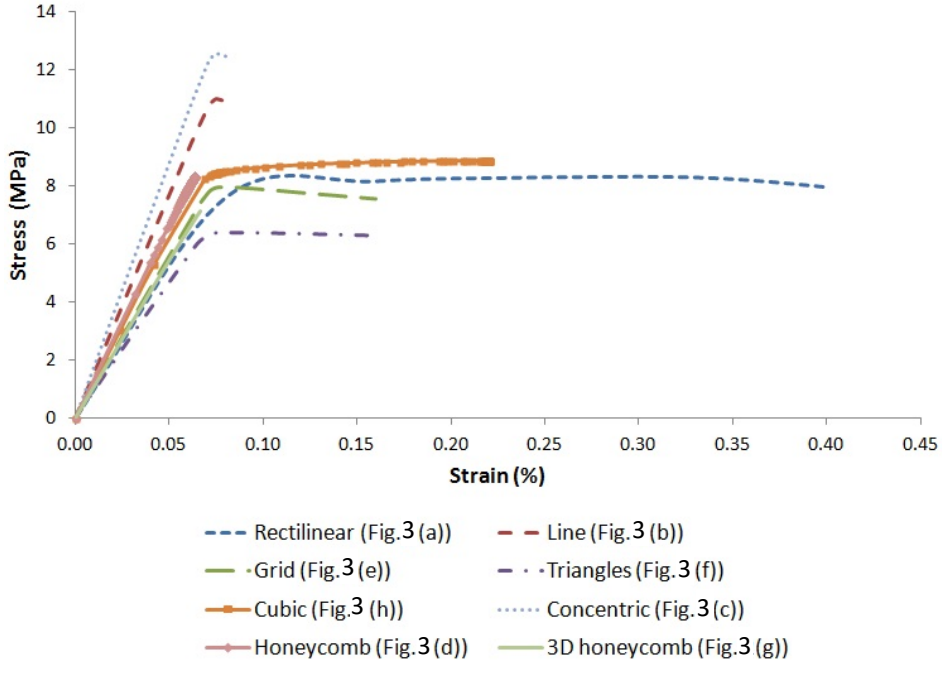

Fig. 7. Stress versus strain for infill density of 30%

Indeed, in order to generate a strain (ε) of 0.075%, it is necessary to apply a stress of 9.4 MPa for the concentric type and only 4.6 MPa for 3D Honeycomb. For the configuration which has only lines parallel to the direction of the load, the strain requires a large loading. On the other hand, for the configuration consisting of a pattern not parallel to the direction of the load, the strain requires less effort. In this phase, the reached ultimate stress is 9.42 MPa for the infill density of 20% and 12.56 MPa for the one of 30%. These results show us that the mechanical characteristics of the curves with 30% infill density are superior to those of the curve with 20% infill density. For the same infill density, we notice that there is a wide range of mechanical response given according to the different infill patterns. This variety comes largely from the discontinuities of material generated by the patterns. In addition, the results show that increasing infill density increased UTS for all levels of infill patterns. This increase could be explained by the reduction in the porosity rate inside the parts manufactured by FDM.

3.1. Taguchi method

From the experimental results presented in Table 2, the ratio (S/N) is calculated to obtain the graph (Fig. 8) of the Taguchi's method. The highest UTS of 12.56 MPa has been obtained for experiments 2.

From Figure 8, we can see a large variation in UTS according to the infill pattern and the infill density. This shows that these two parameters have a significant effect on the UTS.

We notice that increasing the infill density has increased the value of the UTS. This trend has been confirmed by literature [8-10, 13]. Indeed, increasing the infill density reduces the air gap between the rasters and therefore increases the number of contacts between the layers and between the rasters. This ensures a strong bond between the rasters in the layers and therefore ensures high mechanical resistance.

Regarding the infill patterns, we notice that the 'concentric' pattern occupies the first position giving a maximum UTS. A similar study confirmed this performance for the case of the 'concentric' pattern [13].

Table 2.
Matrix of experiments and experimental results using Taguchi method

Experiment number	Factors		UTS, MPa
	A	B	
1	Concentric	20	9.4240
2	Concentric	30	12.5659
3	Line	20	7.8535
4	Line	30	10.9952
5	Cubic	20	7.8050
6	Cubic	30	8.8603
7	Rectilinear	20	5.7242
8	Rectilinear	30	8.3321
9	Honeycomb	20	8.2866
10	Honeycomb	30	8.3238
11	3D Honeycomb	20	4.7697
12	3D Honeycomb	30	7.1420
13	Grid	20	6.3304
14	Grid	30	7.9403
15	Triangles	20	6.3403
16	Triangles	30	6.4142

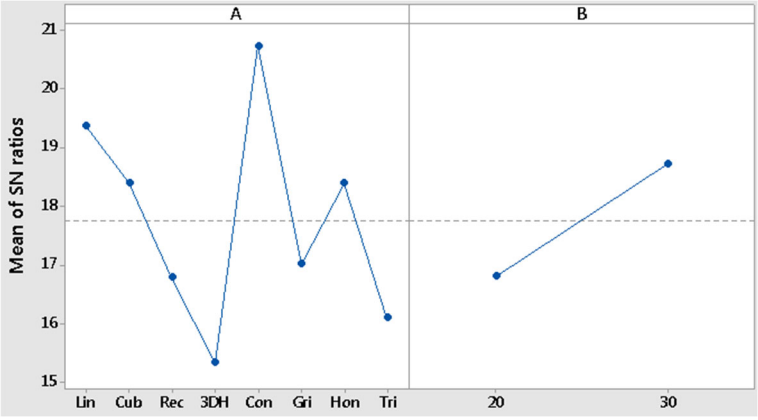

Fig. 8. Main effects plot for S/N ratio

Table 3.
Analysis of variance (ANOVA)

Source	DoF	Sum of squares	Mean Squares	Fisher value	Pr(>F)	Contribution, %
Infill pattern	7	39.363	5.6233	7.00	0.010	68.69
Infill density	1	12.320	12.3204	15.34	0.006	21.49
Error	7	5.621	0.8030			
Total	15	57.305				

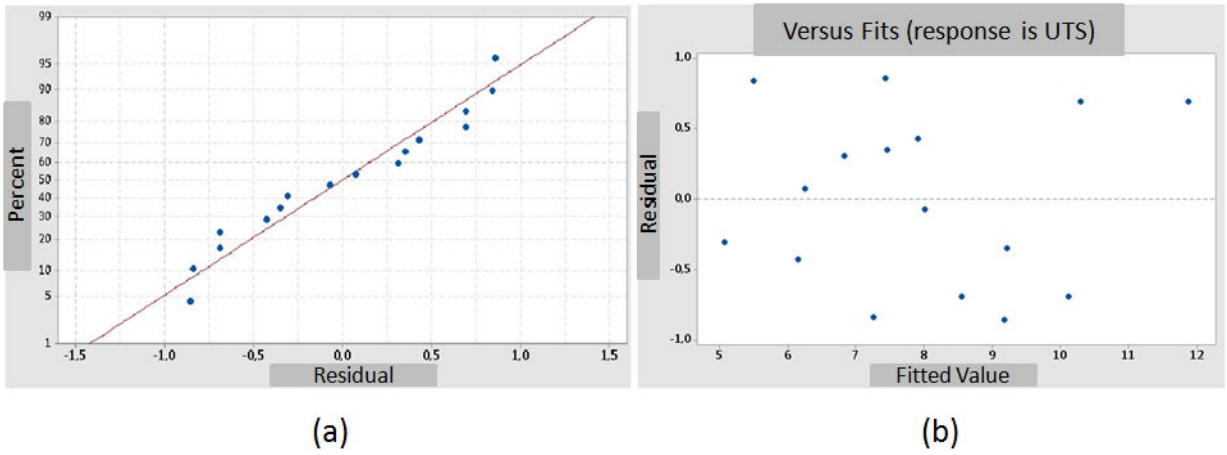

Fig. 9. a) Normal probability plot and b) residue analysis

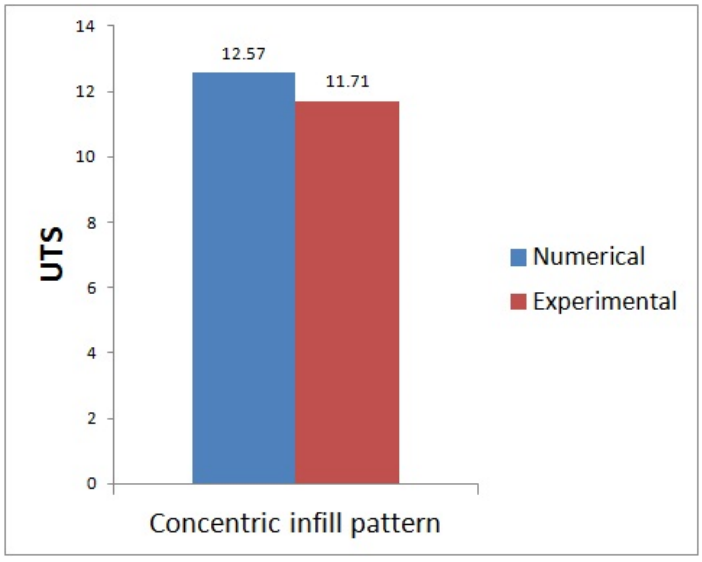

Fig. 10. Numerical results of the maximum UTS for both digital and physical test specimens

For the other infill patterns, we observe a big difference between the values of the UTS. This very marked difference in stress values comes largely from the material discontinuities generated by the patterns.

3.2. Analysis of variance (ANOVA)

In Figure 9a, we observe that the residuals approximately follow a straight line. Therefore, we have a normal

distribution of the residuals. In addition, the residues are distributed at random (Fig. 9b). Therefore, the analysis of the residues does not reveal any remarkable dispositions.

ANOVA results (Tab. 3) show that the significant factors are the infill pattern and the infill density since their p-value (probability value) is less than 0.05. This result is confirmed by those obtained by Yadav et al. and Dave et al. [2,13]. In addition, the infill pattern has the greatest contribution that is 68.69%.

3.3. Validation of numerical results

In order to study the validity of our numerical results, we have deferred in the Figure 10, the values of the UTS obtained numerically and experimentally for the two test specimens physical and numerical. These values are obtained using a combination of the two parameters which give the maximum UTS, i.e. the concentric infill pattern and the infill density of 30%.

According to this graph, we can see that the numerical value of UTS is greater than the experimental one. Indeed, the digital test specimen is more rigid than the experimental one since the first one has no geometric defect and has a perfect 'inter-raster' connection [19].

The difference between numerical and experimental value is 6.8%. In the field of 3D printing, this deviation can be considered acceptable.

4. Conclusions

In this study, modelling the test specimens from a G-code file have been fully automated, and the effect of the infill patterns and the infill density on their mechanical tensile behaviour has been studied using a Taguchi NDoE. From this approach, many infill patterns have been tested, and the significant parameters have been determined. We have found that the 'concentric' infill pattern provides the best mechanical strength followed by the 'line' infill pattern. Our results showed that the infill and the density pattern have significant effects and that the infill pattern has the greatest contribution which is 68.69%. From our bibliographic study, we can confirm that in this study, the NDoE method was used for the first time by the mesostructured approach. This approach allowed us to considerably minimize the cost of the experiments while obtaining a 6.8% difference between the numerical and experimental values of the UTS. Finally, this study provided an important modelling tool for the design and manufacture of functional parts and elucidated the effect of various infill patterns on the tensile properties of the test specimens.

References

[1] J. Taczała, W. Czepułkowska, B. Konieczny, J. Sokołowski, M. Kozakiewicz, P. Szymor, Comparison of 3D printing MJP and FDM technology in dentistry, Archives of Materials Science and Engineering 101/1 (2020) 32-40. DOI: https://doi.org/10.5604/01.3001.0013.9504

[2] D.K. Yadav, R. Srivastava, S. Dev, Design and fabrication of ABS part by FDM for automobile application, Materials Today: Proceedings 26 (2020) 2089-2093. DOI: https://doi.org/10.1016/j.matpr.2020.02.451

[3] T. Sathies, P. Senthil, M.S. Anoop, A review on advancements in applications of fused deposition modelling process, Rapid Prototyping Journal 26/4 (2020) 669-687. DOI: https://doi.org/10.1108/RPJ-08-2018-0199

[4] O.A. Mohamed, S.H. Masood, J.L. Bhowmik, Optimization of fused deposition modeling process parameters for dimensional accuracy using I-optimality criterion, Measurement 81 (2016) 174-196. DOI: https://doi.org/10.1016/j.measurement.2015.12.011

[5] J.M. Chacon, M.A. Caminero, E. Garcla-Plaza, P.J. Nunez, Additive manufacturing of PLA structures using fused deposition modelling: Effect of process parameters on mechanical properties and their optimal selection, Materials and Design 124 (2017) 143-157. DOI: https://doi.org/10.1016/j.matdes.2017.03.065

[6] M. Samykano, S.K. Selvamani, K. Kadirgama, W.K. Ngui, G. Kanagaraj, K. Sudhakar, Mechanical property of FDM printed ABS: influence of printing parameters, The International Journal of Advanced Manufacturing Technology 102/9 (2019) 2779-2796. DOI: https://doi.org/10.1007/s00170-019-03313-0

[7] V.H. Nguyen, T.N. Huynh, T.P. Nguyen, T.T. Tran, Single and Multi-objective Optimization of Processing Parameters for Fused Deposition Modeling in 3D Printing Technology, International Journal of Automotive and Mechanical Engineering 17/1 (2020) 7542-7551. DOI: https://doi.org/10.15282/ijame.17.1.2020.03.0558

[8] M. Fernandez-Vicente, W. Calle, S. Ferrandiz, A. Conejero, Effect of infill parameters on tensile

mechanical behavior in desktop 3D printing, 3D Printing and Additive Manufacturing 3/3 (2016) 183-192. DOI: https://doi.org/10.1089/3dp.2015.0036

[9] K.L. Alvarez C, R.F. Lagos C, M. Aizpun, Investigating the influence of infill percentage on the mechanical properties of fused deposition modelled ABS parts, Ingenieria e Investigacion 36/3 (2016) 110-116. DOI: https://doi.org/10.15446/ing.investig.v36n3.56610

[10] A. Qattawi, B. Alrawi, A. Guzman, Experimental optimization of fused deposition modelling processing parameters: a design-for-manufacturing approach, Procedia Manufacturing 10 (2017) 791-803. DOI: https://doi.org/10.1016/j.promfg.2017.07.079

[11] X. Zhou, S.-J. Hsieh, C.-C. Ting, Modelling and estimation of tensile behaviour of polylactic acid parts manufactured by fused deposition modelling using finite element analysis and knowledge-based library, Virtual and Physical Prototyping 13/3 (2018) 177-190. DOI: https://doi.org/10.1080/17452759.2018.1442681

[12] C. Lubombo, M.A. Huneault, Effect of infill patterns on the mechanical performance of lightweight 3D-printed cellular PLA parts, Materials Today: Communications 17 (2018) 214-228. DOI: https://doi.org/10.1016/j.mtcomm.2018.09.017

[13] H.K. Dave, N.H. Patadiya, A.R. Prajapati, S.R. Rajpurohit, Effect of infill pattern and infill density at varying part orientation on tensile properties of fused deposition modeling-printed poly-lactic acid part, Proceedings of the Institution of Mechanical Engineers, Part C: Journal of Mechanical Engineering Science 235/10 (2021) 1811-1827. DOI: https://doi.org/10.1177/0954406219856383

[14] ASTM D3039/D3039M-00: Standard test method for tensile properties of polymer matrix composite materials, in: Annual Book of ASTM Standards Volume 15.03, American Society for Testing and Materials, West Conshohocken, PA, 2000. DOI: https://doi.org/10.1520/D3039_D3039M-00

[15] F. Górski, W. Kuczko, R. Wichniarek, A. Hamrol, Computation of Mechanical Properties of Parts Manufactured by Fused Deposition Modeling Using Finite Element Method, in: Á. Herrero, J. Sedano, B. Baruque, H. Quintián, E. Corchado (eds.), 10th International Conference on Soft Computing Models in Industrial and Environmental Applications. Advances in Intelligent Systems and Computing, Vol. 368, Springer, Cham, 2015, 403-413. DOI: https://doi.org/10.1007/978-3-319-19719-7_35

[16] S. Naghieh, M.R. Karamooz Ravari, M. Badrossamay, E. Foroozmehr, M. Kadkhodaei, Numerical investigation of the mechanical properties of the additive manufactured bone scaffolds fabricated by FDM: The effect of layer penetration and post-heating, Journal of the Mechanical Behavior of Biomedical Materials 59 (2016) 241-250. DOI: https://doi.org/10.1016/j.jmbbm.2016.01.031

[17] M. Othmani, A. Chouaf, K. Zarbane, Modeling and numerical analysis of the mechanical behavior of parts obtained by the FDM type additive manufacturing process, Proceedings of the Mediterranean Symposium on Smart City Application "SCAMS'17", Tangier, Morocco, 2017, Article no. 3, pp. 1-4. DOI: https://doi.org/10.1145/3175628.3175654

[18] P.J. Baikerikar, C.J. Turner, Comparison of as-built FEA simulations and experimental results for additively manufactured dogbone geometries. Proceedings of the ASME 2017 International Design Engineering Technical Conferences and Computers and Information in Engineering Conference, Volume 1: 37th Computers and Information in Engineering Conference, Cleveland, Ohio, USA, 2017. Article no. V001T02A021. DOI: https://doi.org/10.1115/DETC2017-67538

[19] M. Othmani, K. Zarbane, A. Chouaf, Enhanced mesostructural modeling and prediction of the mechanical behavior of acrylonitrile butadiene styrene parts manufactured by fused deposition modeling, International Review of Mechanical Engineering 14/4 (2020) 243-252. DOI: https://doi.org/10.15866/ireme.v14i4.17736

[20] S-H. Ahn, M. Montero, D. Odell, S. Roundy, P.K. Wright, Anisotropic Material Properties of Fused Deposition Modeling ABS, Rapid Prototyping Journal 8/4 (2002) 248-257. DOI: https://doi.org/10.1108/13552540210441166

[21] T.J. Gordelier, P.R. Thies, L. Turner, L. Johanning, An Optimising the FDM additive manufacturing process to achieve maximum tensile strength: a state-of-the-art review, Rapid Prototyping Journal 25/6 (2019) 953-971. DOI: https://doi.org/10.1108/RPJ-07-2018-0183

[22] D.M. Patel, Effects of infill patterns on time, surface roughness and tensile strength in 3D printing, International Journal of Engineering Development and Research 5/3 (2017) 566-569.

[23] A. Alafaghani, A. Qattawi, Investigating the effect of fused deposition modeling processing parameters using

Taguchi design of experiment method, Journal of Manufacturing Processes 36 (2018) 164-174. DOI: https://doi.org/10.1016/j.jmapro.2018.09.025

[24] A. Pandzic, D. Hodzic, A. Milovanovic, Effect of infill type and density on tensile properties of PLA material for FDM process, Proceedings of the 30th DAAAM International Symposium on Intelligent Manufacturing and Automation, Vienna, Austria, 2019, 0545-0554. DOI: https://doi.org/10.2507/30th.daaam.proceedings.074

[25] A. Chadha, M.I.U. Haq, A. Raina, R.R. Singh, N.B. Penumarti, M.S. Bishnoi, Effect of fused deposition modelling process parameters on mechanical properties of 3D printed parts, World Journal of Engineering 16/4 (2019) 550-559. DOI: https://doi.org/10.1108/WJE-09-2018-0329

[26] G. Ehrmann, A. Ehrmann, Shape-Memory Properties of 3D Printed PLA Structures. Shape-Memory Properties of 3D Printed PLA Structures, Proceedings 69/1 (2021) 6. DOI: https://doi.org/10.3390/CGPM2020-07198

[27] A. Garg, A. Bhattacharya, An insight to the failure of FDM parts under tensile loading: finite element analysis and experimental study, International Journal of Mechanical Sciences 120 (2017) 225-236. DOI: https://doi.org/10.1016/j.ijmecsci.2016.11.032

[28] A. Schmailzl, T. Amann, M. Glockner, M. Fadanelli, M. Wagner, S. Hierl, Finite element analysis of thermoplastic probes under tensile load using LS-DYNA compared to ANSYS WB 14 in correlation to experimental investigations, Proceedings of the ANSYS Conference & 30th CADFEM users' meeting, Kassel, 2012.